Reprint 2017-9

Impact of Canopy Representations on Regional Modeling of Evapotranspiration using the WRF-ACASA Coupled Model

Liyi Xu, Rex David Pyles, Kyaw Tha Paw U, Richard Snyder,
Erwan Monier, Matthias Falk and Shu-Hua Chen

Reprinted with permission from *Agricultural and Forest Meteorology*, 247: 79–92.

The **MIT Joint Program on the Science and Policy of Global Change** combines cutting-edge scientific research with independent policy analysis to provide a solid foundation for the public and private decisions needed to mitigate and adapt to unavoidable global environmental changes. Being data-driven, the Joint Program uses extensive Earth system and economic data and models to produce quantitative analysis and predictions of the risks of climate change and the challenges of limiting human influence on the environment—essential knowledge for the international dialogue toward a global response to climate change.

To this end, the Joint Program brings together an interdisciplinary group from two established MIT research centers: the **Center for Global Change Science (CGCS)** and the **Center for Energy and Environmental Policy Research (CEEPR)**. These two centers—along with collaborators from the Marine Biology Laboratory (MBL) at Woods Hole and short- and long-term visitors—provide the united vision needed to solve global challenges.

At the heart of much of the program's work lies MIT's Integrated Global System Model. Through this integrated model, the program seeks to discover new interactions among natural and human climate system components; objectively assess uncertainty in economic and climate projections; critically and quantitatively analyze environmental management and policy proposals; understand complex connections among the many forces that will shape our future; and improve methods to model, monitor and verify greenhouse gas emissions and climatic impacts.

This reprint is intended to communicate research results and improve public understanding of global environment and energy challenges, thereby contributing to informed debate about climate change and the economic and social implications of policy alternatives.

—Ronald G. Prinn and John M. Reilly,
Joint Program Co-Directors

MIT Joint Program on the Science and Policy of Global Change

Massachusetts Institute of Technology
77 Massachusetts Ave., E19-411
Cambridge MA 02139-4307 (USA)

T (617) 253-7492 F (617) 253-9845
globalchange@mit.edu
http://globalchange.mit.edu

Agricultural and Forest Meteorology 247 (2017) 79–92

Contents lists available at ScienceDirect

Agricultural and Forest Meteorology

journal homepage: www.elsevier.com/locate/agrformet

Research paper

Impact of canopy representations on regional modeling of evapotranspiration using the WRF-ACASA coupled model

Liyi Xu[a,*], Rex David Pyles[b], Kyaw Tha Paw U[b], Richard Snyder[b], Erwan Monier[a], Matthias Falk[b], Shu-Hua Chen[b]

[a] Joint Program on the Science and Policy of Global Change, Massachusetts Institute of Technology, Cambridge, MA, USA
[b] Department of Land, Air, and Water Resources, University of California Davis, Davis, CA, USA

ARTICLE INFO

Keywords:
Land surface modeling
WRF
Canopy representation
Regional modeling
Reference evapotranspiration
Actual evapotranspiration

ABSTRACT

In this study, we couple the Weather Research and Forecasting Model (WRF) with the Advanced Canopy-Atmosphere-Soil Algorithm (ACASA), a high complexity land surface model, to investigate the impact of canopy representation on regional evapotranspiration. The WRF-ACASA model uses a multilayer structure to represent the canopy, consequently allowing microenvironmental variables such as leaf area index (LAI), air and canopy temperature, wind speed and humidity to vary both horizontally and vertically. The improvement in canopy representation and canopy-atmosphere interaction allow for more realistic simulation of evapotranspiration on both regional and local scales. The coupled WRF-ACASA model is compared with the widely used intermediate complexity Noah land surface model in WRF (WRF-Noah) for both potential (ETo) and actual evapotranspiration (ETa). Two LAI datasets (USGS and MODIS) are used to study the model responses to surface conditions. Model evaluations over a diverse surface stations from the CIMIS and AmeriFlux networks show that an increase surface representations increase the model accuracy in ETa more so than ETo. Overall, while the high complexity of WRF-ACASA increases the realism of plant physiological processes, the model sensitivity to surface representation in input data such as LAI also increases.

1. Introduction

The land surface is an important component that contributes to the evolution of atmospheric processes. Complex interactions between the atmosphere and land surface drive the impacts of energy, momentum, heat, water, and gas exchanges on atmospheric motions. Many of these effects are attributed to the presence of vegetation in the surface layer (Potter et al., 1993; Dickinson and Henderson-Sellers, 2006; Dirmeyer et al., 2010), which is a crucial part of the land surface layer, representing 99% of the mass of surface biota. Because of this, land surface parameterization in atmospheric models must emphasize the processes associated with vegetation. Effects of climate on vegetation phenology have long been a research focus in the ecology and plant science communities (Levitt et al., 1980; Jones, 1992). Climate conditions such as temperature, humidity, and radiation strongly influence plant physiological responses in photosynthesis, respiration, transpiration, and energy flux. However, the influences of vegetation on the climate and atmospheric processes are not as well understood due to numerical complexity and related challenges that arise from properly representing exchanges between the physiologically active vegetated land surfaces and the atmosphere. In recent years, research interests in land and atmospheric interactions have grown considerably, benefitting from the developments of atmosphere and land surface models as well as advanced instrumentation and field campaigns.

Land cover type and vegetation amount are related factors that characterize biosphere-atmosphere interactions. Differences in land use cover can dramatically influence land surface processes by altering surface roughness, canopy transmission of light, physiological responses to environmental controls, and interception of precipitation. Vegetation amount is quantified with the leaf area index (LAI), which is a representation of the total leaf area over a given area of land. Leaves provide surface area for photosynthesis, respiration, and transpiration that control the moisture and energy exchanges with the atmosphere. Specifically, the LAI strongly influences the amount of absorbed solar radiation and its partitioning into sensible and latent energy fluxes. Studies using General Circulation Models (GCMs) have demonstrated the importance and influence of LAI on the short- and long-term evolution of surface hydrology, including snowpack evolution, soil wetness, and evapotranspiration (ET) (Chase et al., 1996; Pitman et al., 1999; Bounoua et al., 2000; Hales et al., 2004). (Gao et al., 2008)

* Corresponding author.
E-mail address: liyixm@mit.edu (L. Xu).

http://dx.doi.org/10.1016/j.agrformet.2017.07.003
Received 8 January 2016; Received in revised form 20 June 2017; Accepted 5 July 2017

further examined the sensitivities of land surface climate to the changes in spatial distribution of LAI from different treatments of surface properties: natural inter-annually varying vegetation versus a 10-year climatological annual cycle. Overall, the study showed that observed inter-annually varying vegetation properties led to improvement in estimations of surface fluxes such as latent heat and surface evapotranspiration, regional surface temperature, and spatial distribution of precipitation.

Actual evapotranspiration (ETa) is the water loss rate by transpiration from plants and evaporation from both soil and vegetation. The standardized Reference evapotranspiration (ETo) is the evaporative loss rate from a virtual 0.15 m tall vegetated surface having known canopy and aerodynamic resistance (Allen et al., 2005). Although ETo is technically defined for a virtual surface, it provides a good estimate of the evapotranspiration from a surface covered by 0.15 m tall cool-season grass with adequate water supply. Vegetation representations of most plants are by definition not directly included in the ETo; however, the response of ETo to environmental variables is closely linked to the response of actual evapotranspiration. The accurate estimations of ETo and ETa are crucial for optimal water management practices and drought monitoring, especially for regions with limited water availability and high water demand, such as the Central Valley of California.

Reference evapotranspiration (ETo) provides a type of environmentally controlled physiological standard model that is useful in assessing potential environmental controls on ETa. In reality, the land surface is covered by diverse vegetation ranging such as grasslands, mixed woodlands, and forests; their existence at any location is a result of the complex interaction of anthropogenic activity, ecological constraints, and environmental controls including water availability. Hence, the ETa commonly differs from the ETo, mainly due to differences in the transpiration component of ET that result from variations in net radiation, aerodynamic resistance to sensible and latent heat transfer, and the bulk surface resistance to water vapor transfer from the surface to the zero plane displacement. The ETa rate ranges from zero up to a potential evapotranspiration (ETc), which is limited by energy availability for vaporizing water. When soil water content is adequate, ETa = ETc, and ETa decreases relative to ETc when soil water (rather than energy availability) limits evapotranspiration.

Transpiration from vegetated surfaces accounts for significant amounts of water entering the atmosphere. In addition to environmental conditions, the canopy vegetation also controls the overall transpiration rate physiologically and physically, by opening and closing stomata to regulate energy and gas exchanges and by making substantial leaf area available for this activity in response to light and water stress. Many processes and interactions in the atmosphere and biosphere influence plant and soil water losses by evapotranspiration. The need to improve representation within surface-atmosphere interactions remains an urgent priority within the modeling community.

Motivated by (Gao et al., 2008) and previous studies, this research extended the earlier works involving coarse resolution GCMs to examine the impacts of land surface representations in regional models (Abramowitz et al., 2008; Henderson-Sellers et al., 1996; Chen et al., 1997). Here, to simulate evapotranspiration over California's diverse terrain and ecosystems, the mesoscale Weather Research and Forecasting model (WRF) is used with two land surface models (LSMs) having two distinct levels of complexity: the intermediate complexity Noah and the complex Advanced Canopy-Atmosphere-Soil Algorithm (ACASA).

The objective of this paper is to investigate how the variability of Reference (ETo) and Actual (ETa) evapotranspiration are influenced by the surface representation, such as leaf area index, and the land surface model complexity. Both ETo and ETa are important for understanding of the hydrologic cycle, vegetation dynamics, and surface energy balances in the surface layer. They are also important variables for use in water management, drought monitoring, agricultural production, and fire hazard management. The effects of leaf area index and model complexity on ETo—which is completely dependent on atmospheric conditions—represents the vegetated controls on the atmosphere that can feedback to the land surface. The simulated ETa includes the feedback processes and represents the complete interaction between the atmosphere and the vegetation.

2. Models, methodology and data

2.1. Models

In this study, the Advanced Research WRF (ARW) model Version 3.1.1 is used to perform climate simulations over California. WRF is a state-of-the-art, mesoscale numerical weather prediction and atmospheric research model developed by a collaborative effort of the National Center for Atmospheric Research (NCAR), the National Oceanic and Atmospheric Administration (NOAA), the Earth System Research Laboratory (ESRL), and many other agencies. The WRF model contains a nearly complete set of compressible and non-hydrostatic equations for atmospheric physics (Chen and Dudhia, 2000). The high spatial and temporal resolution of the WRF model is essential for simulating climate over the intricate terrains and land covers of California. The physical parameterizations used in this study are described in more detail in (Xu et al., 2014).

The land surface models used in this study are the Noah model (Mahrt and Ek, 1984; Chen and Dudhia, 2000) and the ACASA model (Meyers, 1985; Meyers and Paw U, 1987; Pyles, 2000; Pyles et al., 2000). The two models differ significantly in the complexity of the representation of plant physiology and biometeorological processes. While Noah is widely used for both climate studies and weather forecasting, it is an intermediate complexity model with multiple soil layers but only a single canopy layer. NOAH also has varying soil moisture thresholds affecting canopy resistance, based on the WRF soil type. It scales the single leaf-based physical and physiological processes to represent the whole canopy using bulk similarity assumptions. The ACASA model is a higher-complexity model that includes many plant physiological and biometeorological processes (i.e., photosynthesis and respiration) that are not represented in the Noah model. It uses multilayer canopy structures and multiple sun angles within each layer to represent the canopy. These subsequently allow variables such as LAI, air and canopy temperature, wind speed and humidity to also vary vertically. The surface layer is divided into 10 canopy layers and 10 above-canopy layers. Within each canopy layer there are 10 leaf angle classes—9 sunlit angle at 10° intervals and 1 shaded—to represent differential illumination of canopy surfaces. ACASA has soil moisture dependence for the bare soil, and for the 10 layers of 10 leaf radiation angle/shaded classes (100 total) the leaf physiology (photosynthesis and stomatal conductance) with a volumetric soil moisture threshold ranging from 0.06 to 0.19, defined by WRF soil type. Soil drier than this threshold creates a graduated effect representing moisture stress, with dependence on how dry the soil is below this threshold. A third order turbulent closure scheme used in the ACASA model allows both down- and counter-gradient transport, which are not presented in the Noah model.

Of particular importance is the role of Leaf Area Index (LAI) in controlling the surface processes in the two land surface models. LAI in the Noah model is primary used to calculate the bulk canopy resistance of the single surface layer. Canopy resistance for vegetation transpiration and energy partitioning is estimated using the Jarvis parameterization, where canopy resistance R_c is a function of R_{c_min} (a single prescribed minimum canopy resistance specified by plant functional type), LAI, and F1, F2, F3, and F4, which account for the effects of radiation, temperature, humidity, and soil moisture (Jacquemin and Noilhan, 1990; Chen and Dudhia, 2001a; Chen and Dudhia, 2001b).

$$R_c = \frac{R_{cmin}}{LAI\,(F_1F_2F_3F_4)} \quad (1)$$

In the ACASA model, LAI is used to create vertical profiles for multilayer canopy structures. Depending on land-use cover, the LAI values affect light and precipitation interception and alter the canopy energy budgets. The model calculates canopy resistance and stomatal resistance at the leaf surface of each vertical layer using a combination of the Ball- Berry stomatal conductance (Leuning, 1990; Collatz et al., 1991) and the (Farquhar and Von Caemmerer, 1982) photosynthesis equation used in (Su et al., 1996).

$$g_{s,w} = m\frac{A_n}{c_s}rh_s + b \tag{2}$$

$$rh_s = \frac{g_b q_A + g_{s,w} q_s(T_L)}{g_b + g_{s,w} q_s(T_L)} \tag{3}$$

$$c_s = c_A - \frac{A_n}{g_b} \tag{4}$$

where $g_{s,w}$ is the leaf stomatal conductance to water vapor, A_n is the net CO_2 uptake rate at the leaf surface, c_s and rh_s are the CO_2 concentration and the fractional relative humidity at the leaf surface, m and b are empirical regression coefficients; c_A is the CO_2 concentration in air, $q_s(T_L)$ is saturated mixing ratio of water vapor at leaf temperature T_L, g_b is the leaf boundary layer conductance, and q_A is the mixing ratio of water vapor in the air. Because evapotranspiration is an inevitable result of plant physiological processes, oversimplifying the linkage between moisture and carbon dioxide fluxes in land surface processes can lead to the loss of vital information that impact climate simulations (Zhan and Kustas, 2001; Houborg and Soegaard, 2004).

2.2. Data

In this study, WRF simulations are forced by the North American Regional Reanalysis (NARR) dataset, which provides input data such as wind speed and direction, temperature, moisture, radiation, and soil temperature to drive the initialization and boundary conditions of the WRF models. The NARR is a regional data set specifically developed for the Northern American region. The temporal and spatial resolutions of this data set are 3-h intervals and 32-km respectively (Mesinger et al., 2006).

Two leaf area index datasets, USGS and MODIS, are used to drive the surface processes. The default USGS LAI data used by the WRF model prescribes the maximum and minimum LAI values for each point according to plant functional types. Monthly LAI is extrapolated linearly between the maximum and minimum LAI values with monthly Green Vegetation Fraction, which is the fraction of the grid cell covered by active vegetation (Gutman and Ignatov, 1998). The MODIS (Moderate Resolution Imaging Spectroradiometer) dataset is measured daily to provide high spatial and temporal resolution LAI (Knyazikhin et al., 1999). The USGS LAI and MODIS LAI are shown in Fig. 1 for different seasons of the year 2006. The USGS LAI values are significantly higher than those of the MODIS LAI dataset, especially during the summer months. There is no interannual variability in the WRF USGS LAI, in contrast to the satellite measured MODIS LAI. Both LAI datasets display temporal and spatial differences among the different time of the year over California.

The main independent observational datasets used to evaluate the model simulations were obtained from the California Irrigation Management Information System (CIMIS) for ETo, and the AmeriFlux network for both ETo and ETa (Fig. 2). The CIMIS stations are sparsely located, mostly in the Central Valley and Southern Coastal areas. All of the CIMIS weather stations are surrounded by irrigated 0.07–0.15 m tall grass with fetch that varies from about 40–100 m. The wind speed is measured at 2.0 m and the temperature and humidity are measured at 1.5 m height. All of the grass fields around the CIMIS stations are irrigated sufficiently frequent to avoid water stress reductions in ET. However, the irrigation frequency and amount are controlled by the property owners and are not recorded. There are only six AmeriFlux sites in California for the study period, even though it is the period with the most active stations, and because some stations are very close by each other, only three distinct markers are visible in Fig. 2. All of the AmeriFlux site have non-irrigated natural vegetation surrounding the stations. Sensor heights are given in Table 1. Moreover, due to the close proximities of the three Sky Oak sites, they are located within the same WRF model grid cell. Therefore, they are not distinguished in the WRF model simulations. The combined coverage of the two datasets still leaves much of California underrepresented for flux observations. Hence, the WRF model can be used as a potentially valuable tool to fill in the temporal and spatial gaps of the surface observations.

In both the ACASA and Noah models, only the dominant vegetation types or plant functional types (PFTs) are used to represent each grid cell. However, sometime these PFTs do not necessarily represent the observed vegetation type at each of the stations, as shown in Table 1. For example, the three Sky Oak sites (USSO2, USSO3, and USSO4) are identified as evergreen needleleaf forest by WRF, instead of the savannas and shrublands that actually surround the sites (observed PFT).

2.3. Model setup

Four model simulations from the combination of the two land surface models and two LAI representations were used to simulate ETo and ETa across all of California's vast and diverse terrains and ecosystems. The four simulations were: WRF-ACASA with default USGS LAI, WRF-ACASA with high resolution MODIS LAI, WRF-Noah with USGS LAI, and WRF-Noah with MODIS LAI. Simulations were performed for the years 2005 and 2006 with horizontal grid spacing of 8 km × 8 km. Each simulation is spun up for 1 month and then ran continuous till the beginning of next year. For example, the simulation for year 2005 starts at December 1st, 2004 and run till January 1, 2006. December 2004 is used for spin up the model. Because NARR and WRF are in Greenwich time (UTC), January 1, 2006 contains the last few hours of 2005 for the local time zone. Besides the differences in the land surface model, all simulations employed the same set of atmospheric physics schemes stemming from the WRF model. These include the Purdue scheme for microphysics (Chen and Sun, 2002), the Rapid Radiative Transfer Model for long wave radiation (Mlawer et al., 1997), the Dudhia scheme for shortwave radiation (Dudhia, 1989), the Monin-Obukhov similarity scheme for surface layer physics of non-vegetated surfaces and the ocean, and the MRF scheme for the planetary boundary layer (Hong and Pan, 1996). WRF runs at a 60-s time step, while the radiation scheme and the land surface schemes are called every 30 min, which is the standard time averaging of eddy covariance method the ACASA model is based on. Boundary and soil conditions are initialized by input forcings from NARR. WRF utilizes an initial soil moisture and soil type map for its domain, including California. Subsequently as WRF and the land surface models are run, the soil moisture is simulated based on the LSM hydrological sub-models that include actual evapotranspiration and water movement within the soil layers; therefore, the soil moisture values in the simulations represent a spatial and temporal matrix of values created by the simulations. Reference evapotranspiration was calculated using the standardized reference evapotranspiration ETo equation from (Allen et al., 2005) with simulated surface air temperature, dew point temperature, solar radiation, and wind speed at 2 m height. Actual evapotranspiration was calculated within the WRF-ACASA and WRF-Noah models.

For the four simulations, ETo and ETa were compared with surface observations to test the hypothesis that terrestrial representations in land surface models influence the simulated evapotranspiration on both local and regional scales. Hourly, daily, monthly and annual temporal scales were used to evaluate the variability of model performance. The comparison between surface observations and model simulations were similar for 2005 and 2006; however, due to the considerable missing observation data during 2005, mainly results from 2006 are presented

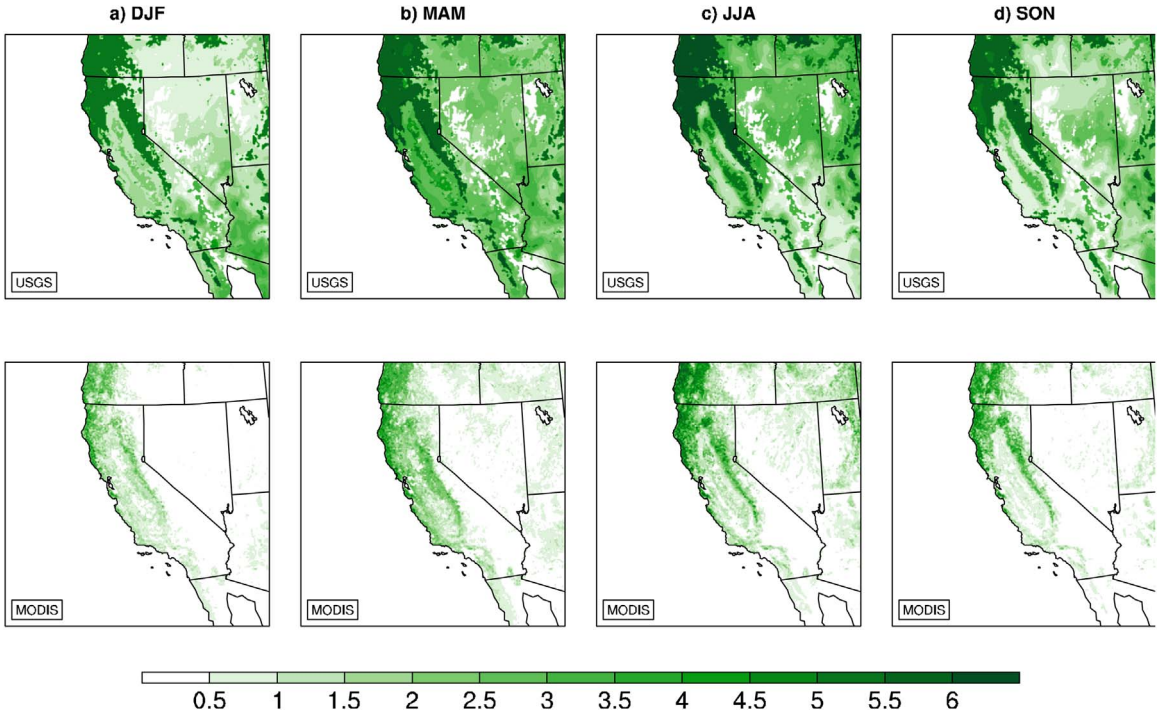

Fig. 1. Maps of MODIS LAI and USGS LAI for a) winter: December, January, and February (DJF); b) spring: March, April, and May (MAM); summer: June, July, and August (JJA); and autumn: September, October, and November (SON) of 2006.

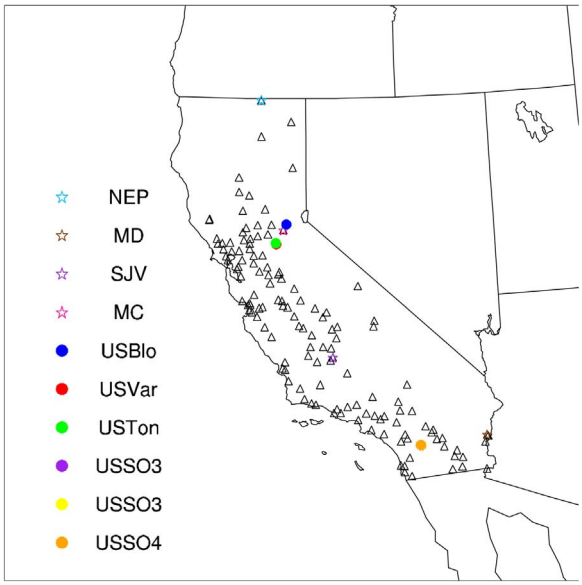

Fig. 2. Maps of the 120 CIMIS stations for reference evapotranspiration (ETo) measurements in triangles, and of the 6 AmeriFlux stations for both reference (ETo) and actual (ETa) evapotranspiration measurements in color dots.

here. While CIMIS stations are irrigated, the ACASA or the Noah model does have the ability to apply irrigation in the form of scheduled precipitation. In addition, the CIMIS site irrigation is controlled by the property owner. The irrigation frequency and amount was not recorded, so it could not be input into the ACASA model.

Some of the challenges in comparing model simulations and the observations are that (1) the measurement heights are sometimes different from the simulated height, and (2) the station landscape could be different from the simulated grid point. The CIMIS stations had measurements heights for air temperature and relative humidity at 1.5 m, and wind speed and radiation at 2 m height. The AmeriFlux sites had their measurements at varying heights, as shown in Table 1, that also includes what heights the model output was for. ETo was calculated for those AmeriFlux heights based on the indicated WRF-ACASA height and the observed heights. The models simulate surface temperature based on a 2 m height. Moreover, this simulated 2 m temperature might be representing the understory of taller plant ecosystems in the WRF-ACASA model (WRF-Noah does not suffer the same problems; because Noah is a big-leaf model, the 2-m height represents a height more similar in characteristics to the observations). In addition, some stations were within patches of specific landscape types that may differ significantly from the assigned overall grid point landscape in WRF. For example, the observed PFT of the three Sky Oak stations from the AmeriFlux data are different from the WRF PFT (Table 1). This mismatch of PFT leads to an additional simulation of WRF-ACASA with MODIS LAI with bias-corrected PFT over the Sky Oaks sites in order to examine the impact of PFT.

3. Results and discussion

3.1. Reference evapotranspiration

The seasonal diurnal patterns of ETo from the four WRF simulations are compared with surface observations from CIMIS stations in Fig. 3 and the AmeriFlux sites in Fig. 4. The seasonal diurnal patterns of the model simulations generally compare well with the surface measurements, and the differences between simulations using USGS LAI and MODIS LAI are small. The Northeast Plateau station (NEP) and the Blodgett Forest site (USBlo), where the observed PFTs match the WRF model, show the best model comparisons. The correct PFT affects the microclimate, so the more accurate PFT means the microclimate is more accurate, so the modeled ETo should be more accurate. However, there will still be discrepancies between the different models' ability to simulate ETo. Net radiation, air temperature and relative humidity are the main variables that affect ETo, and the more accurate WRF-ACASA tends to simulate these values more accurately than WRF-Noah. However, in the Mojave Desert (MD), San Joaquin Valley (SJV) and Mountain County (MC) stations, where the observed PFTs do not match well with the model plant functional types, both models overestimate

Table 1
Selected sites from the CIMIS (NEP, MD, SJV, MC) and AmeriFlux (USBLO, USVAR, USTON, SUSO2, USSO3, USSO4) network are compared for height and Plant Functional Type (PFT). The height corresponds to the canopy height in WRF-ACASA, and the height of the station measurement.

Station	Site Name	PFT		Height (m)	
		WRF	Observed	WRF-ACASA	Observed
NEP	Northeast Plateau	Grassland	Irrigated Grassland	1	1.5
MD	Mojave Desert	Shrublands	Irrigated Grassland	3	1.5
SJV	San Joaquin Valley	Irrigated Cropland and Pasture	Irrigated Grassland	1.5	1.5
MC	Sierra Nevada Mountain	Evergreen Needleleaf Forest	Irrigated Grassland	17	1.5
USBLO	Blodgett Forest	Evergreen Needleleaf Forest	Evergreen Needleleaf Forest	17	12.5
USVAR	Vaira Ranch	Savanna	Grassland	10	1
USTON	Tonzi Ranch	Savanna	Woody Savannas	10	23
USSO2	Sky Oak Old	Evergreen Needleleaf Forest	Woody Savannas	17	4.2
USSO3	Sky Oak Young	Evergreen Needleleaf Forest	Closed Shrublands	17	1
USSO4	Sky Oak New	Evergreen Needleleaf Forest	Closed Shrublands	17	15

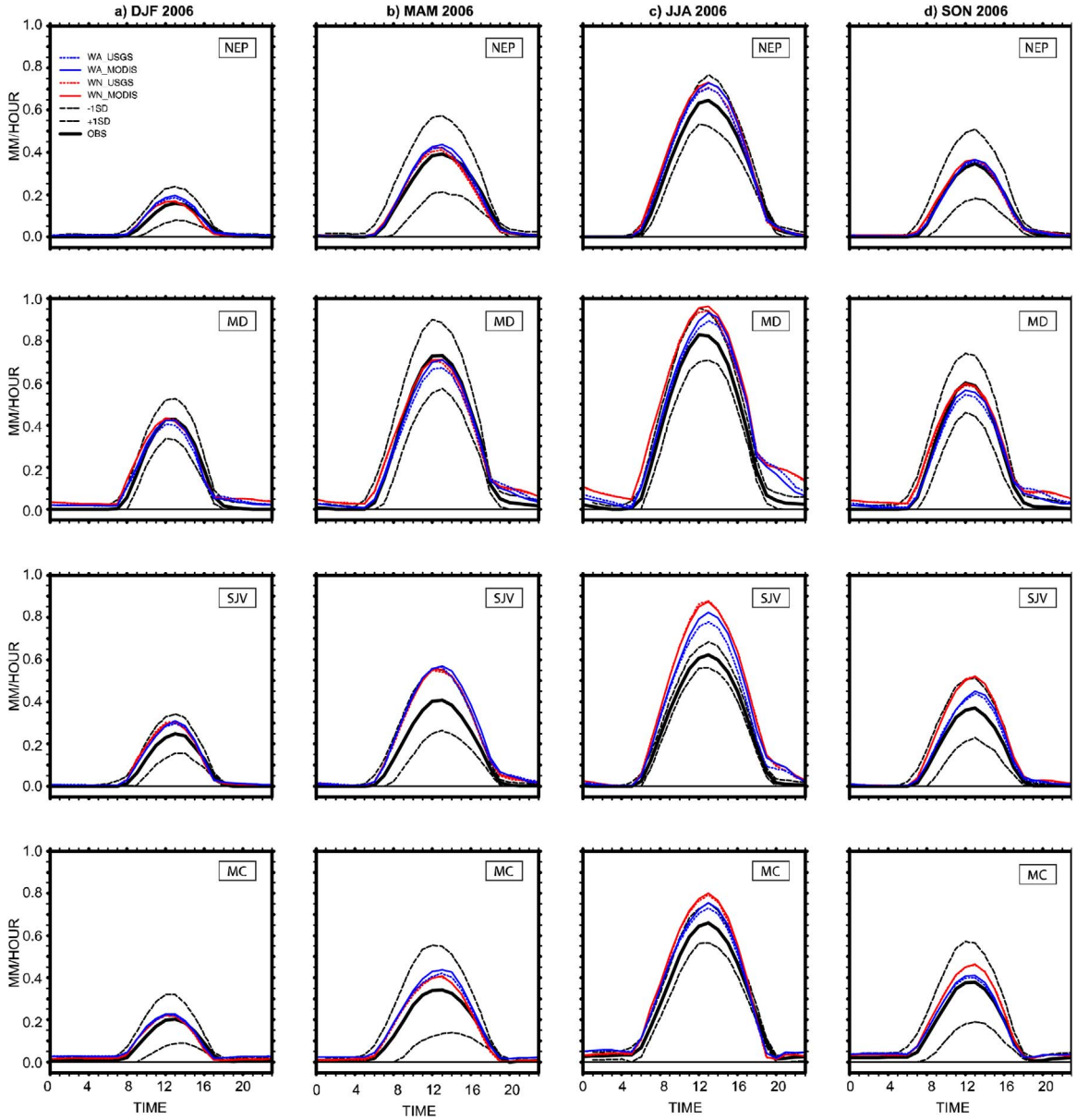

Fig. 3. Seasonal diurnal patterns of reference ETo for the four model simulations for the CIMIS stations during 2006. The thick black lines are CIMIS ETo measurements with two dash lines representing one standard deviation above and below the mean diurnal patterns. The red lines are WRF-Noah simulations and the blue lines are WRF-ACASA simulations. The red and blue dashed lines are for simulations with USGS LAI and the solid lines are for simulations with MODIS LAI. Winter is assumed to be December, January, and February (DJF); spring is March, April, and May (MAM); summer is June, July, and August (JJA); and autumn is September, October, and November (SON).

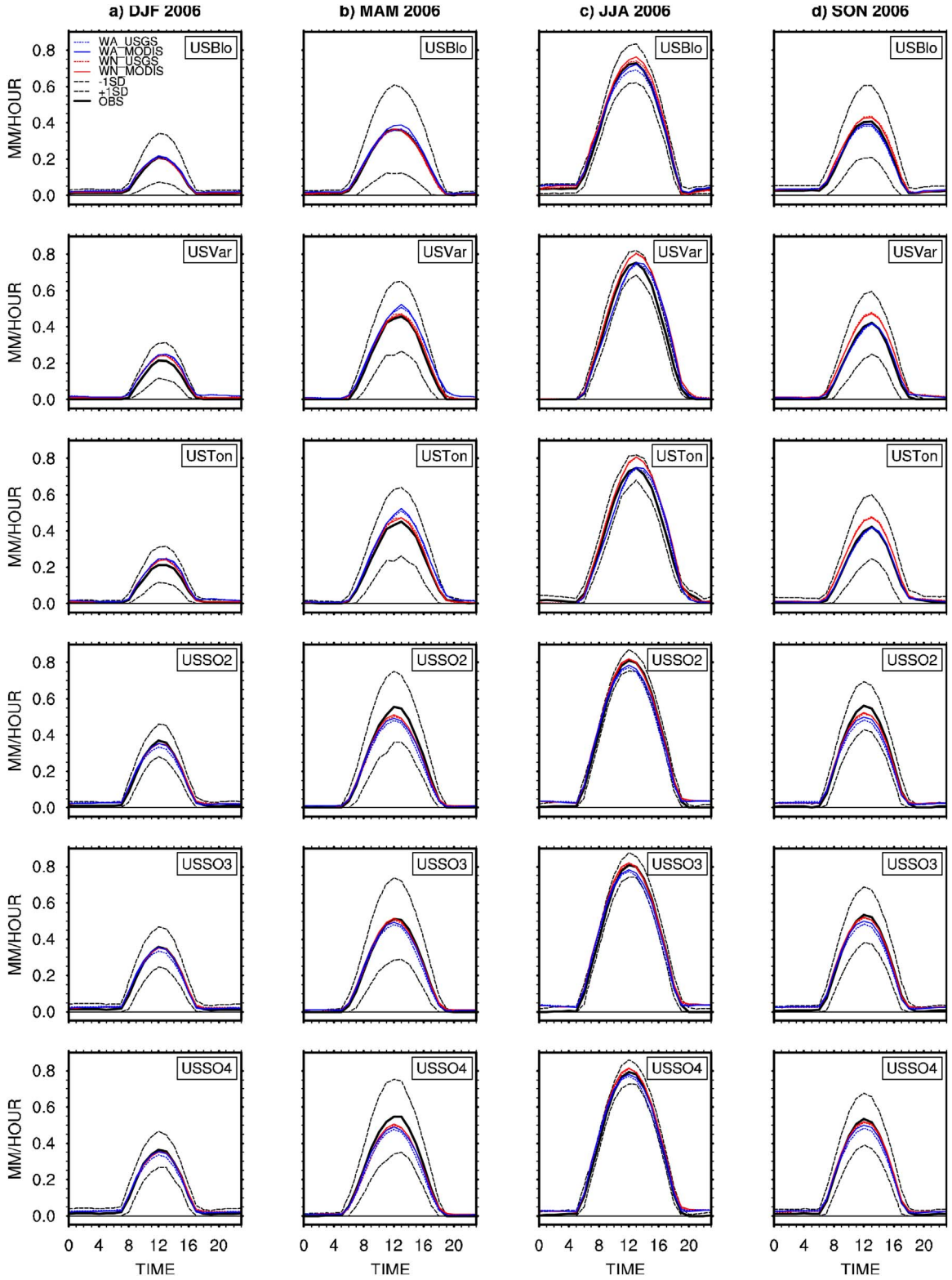

Fig. 4. Seasonal diurnal patterns of reference ETo for the AmeriFlux sites during 2006.The black lines are observed ETo with two dash lines representing one standard deviation away from the mean. The red lines are WRF-Noah simulations and the blue lines are WRF-ACASA simulations. The color dashed lines are for simulations with USGS LAI and the color solid lines are for simulations with MODIS LAI. Winter is (DJF), spring is (MAM), summer is (JJA), and autumn is (SON).

the ETo values during daytime of the warmer seasons. CIMIS ETo is estimated using weather data measured over irrigated grass, and WRF weather data are not from data over irrigated grass. It likely explains the differences between CIMIS and the models. That idea is reinforced by the fact that differences are biggest in the summer months when the difference between weather data over irrigated grass and data from the models is the most different. The two different LAI datasets do not have a significant impact on the ETo simulations at sub daily scale, though usage of the MODIS LAI improve the RMSE of WRF-ACASA simulations for the San Joaquin Valley station by 0.26 mm/day. Overall, the WRF-

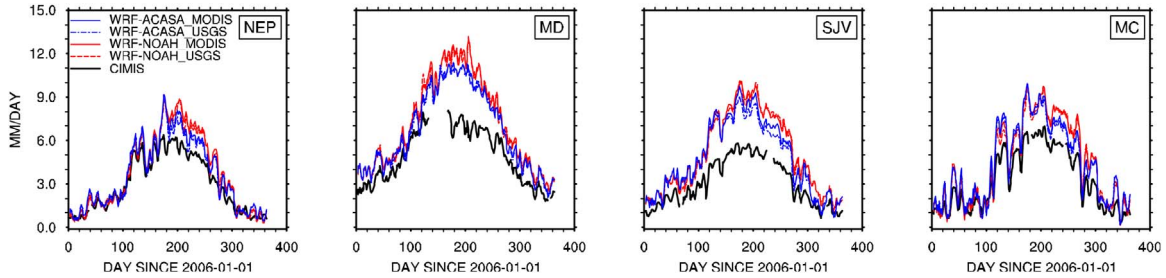

Fig. 5. Time series of reference evapotranspiration for the CIMIS stations. The solid black line represents observation. The blue lines are for WRF-ACASA, and the red lines are for WRF-Noah. The color solid lines are simulations with MODIS LAI, and the color dashed lines are simulations with USGS LAI.

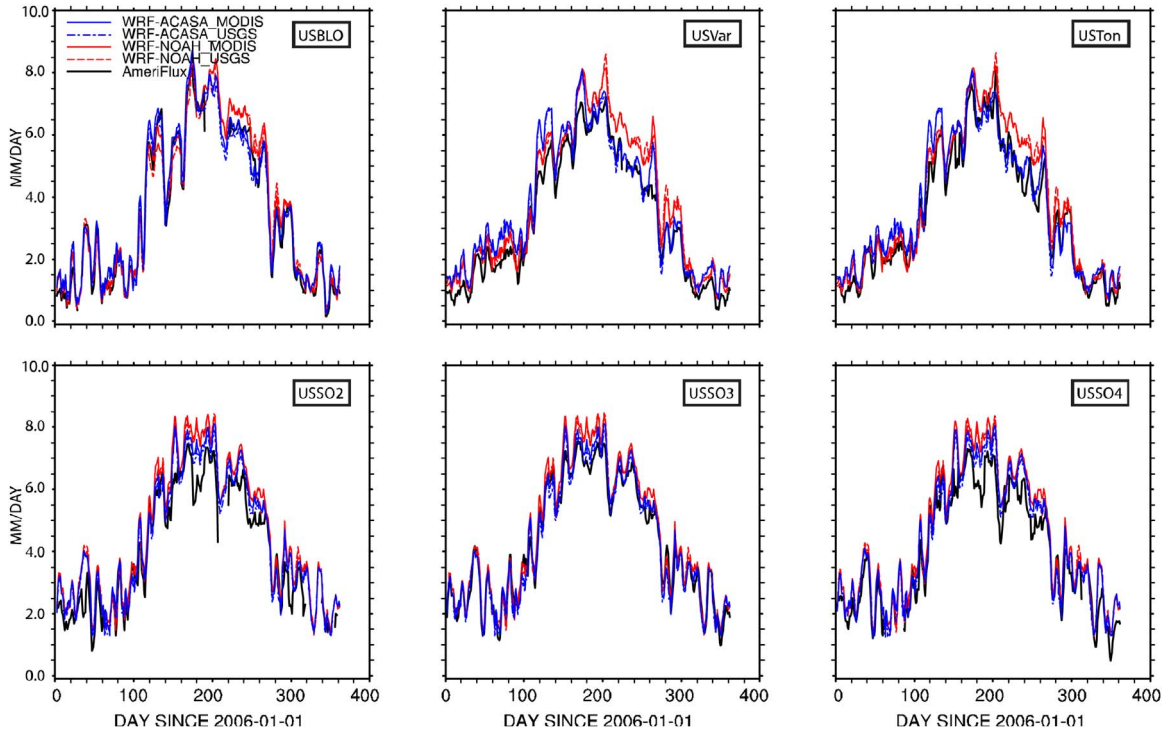

Fig. 6. Time series of reference evapotranspiration for the AmeriFlux sites. The solid black line represents observation. The blue lines are for WRF-ACASA, and the red lines are for WRF-Noah. The solid lines are simulations with MODIS LAI, and the dashed lines are simulations with USGS LAI.

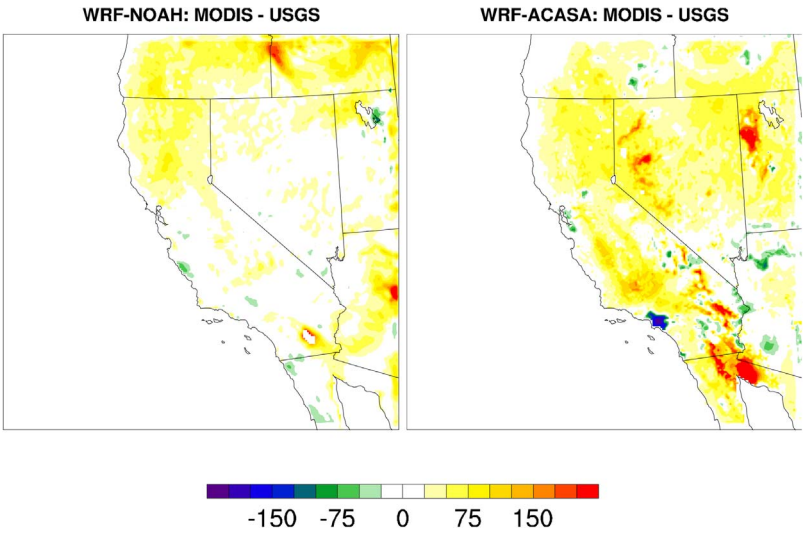

Fig. 7. Maps of cumulative difference in ETo (mm/yr) between MODIS and USGS LAI simulated by WRF-ACASA and WRF-Noah for 2006. The left panel is the differences in WRF-Noah simulations and the right panel is WRF-ACASA simulations.

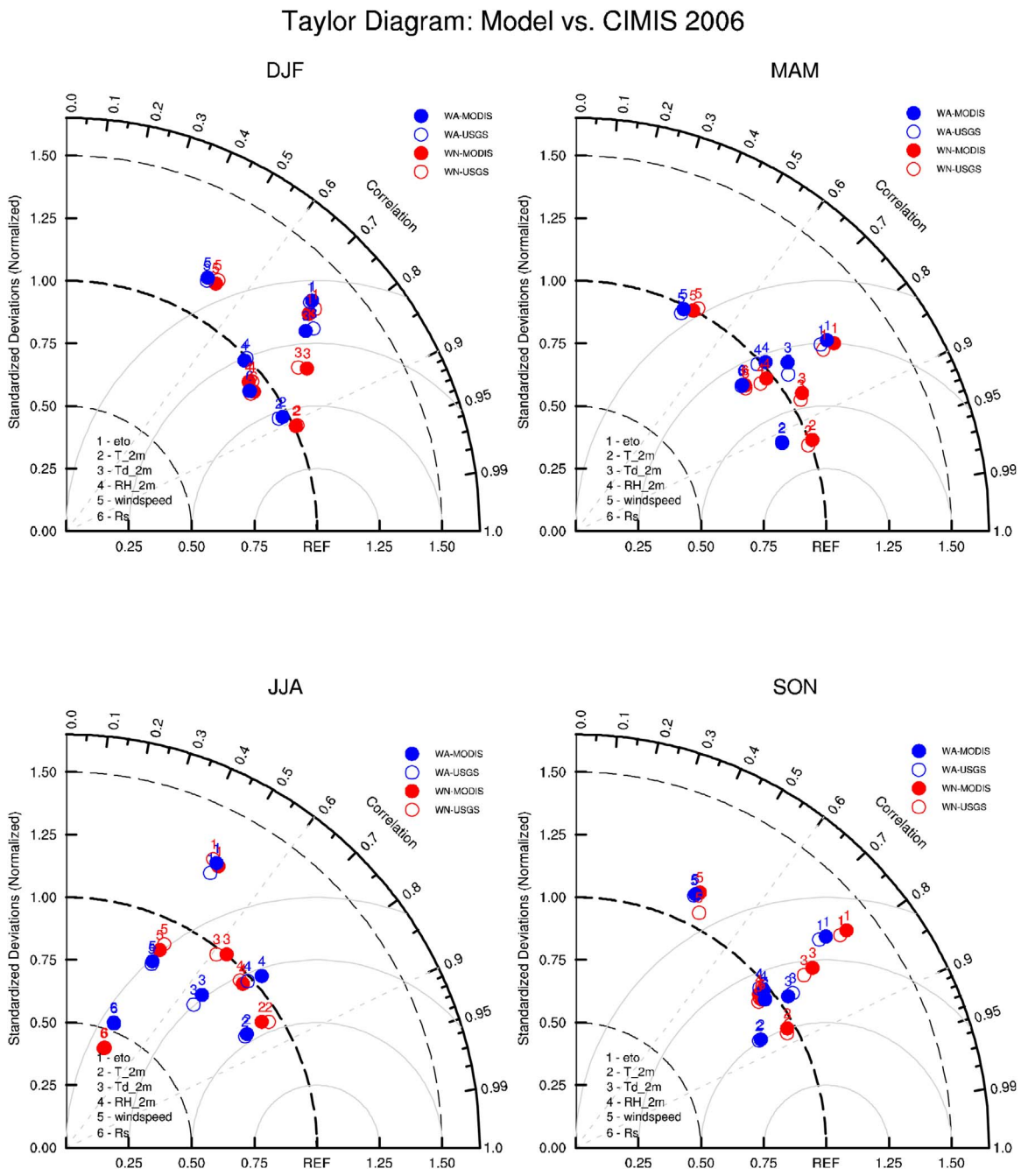

Fig. 8. Seasonal Taylor Diagram for the four WRF simulations vs. CIMIS station measurements for daily ETo, 2 m temperature (T_2 m), dew point temperature (Td_2 m), wind speed (windspeed), and solar radiation (Rs). Blue represents WRF-ACASA simulations, red represents WRF-Noah, open circles are simulations using USGS LAI, and solid dots are simulations using MODIS LAI. Winter is DJF, spring is MAM, summer is JJA, and autumn is SON.

ACASA model results exhibit a reduced bias during the daytime by 0.18 mm/day. Overall, the differences between the two models are not statistically significant and they are both well within the 1 standard deviation of the observed values.

The time series of the daily ETo from the 2006 CIMIS surface observations as well as the four model simulations are compared in Fig. 5. In general, model simulations of daily ETo agree with observations during the cool season but depart from the observed trend during the warmer seasons. The overestimation of daily ETo in the time series are results of the daytime bias in ETo (Fig. 3). These small biases, in the order of a few tenths of a millimeter per hour during the daytime, aggregate to be more pronounced in daily values. The sparsely vegetated Mojave Desert and San Joaquin Valley stations are most problematic for the model simulations and experience the most bias overall. These differences are likely due to the collection of CIMIS weather data over irrigated grass.

Fig. 6 compares the observed and simulated time series of daily ETo in 2006 for the AmeriFlux sites. In Fig. 6, the timing and magnitude of the simulations agrees well with the surface observations for all sites with small differences over the Varia and Tonzi ranches. This reaffirms the results shown in Fig. 4, which shows simulated diurnal patterns of ETo. The more complex WRF-ACASA model reduces the ETo bias over Vaira and Tonzi Ranch stations in summer and autumn in both hourly and daily scales by about 0.13 mm/day. This is may result from more sophisticated dew point temperature in the WRF-ACASA model where higher complexity in plant physiology representation and multilayer canopy structure improve the moisture exchange within and above the canopy, as shown in (Xu et al., 2014). However, the differences

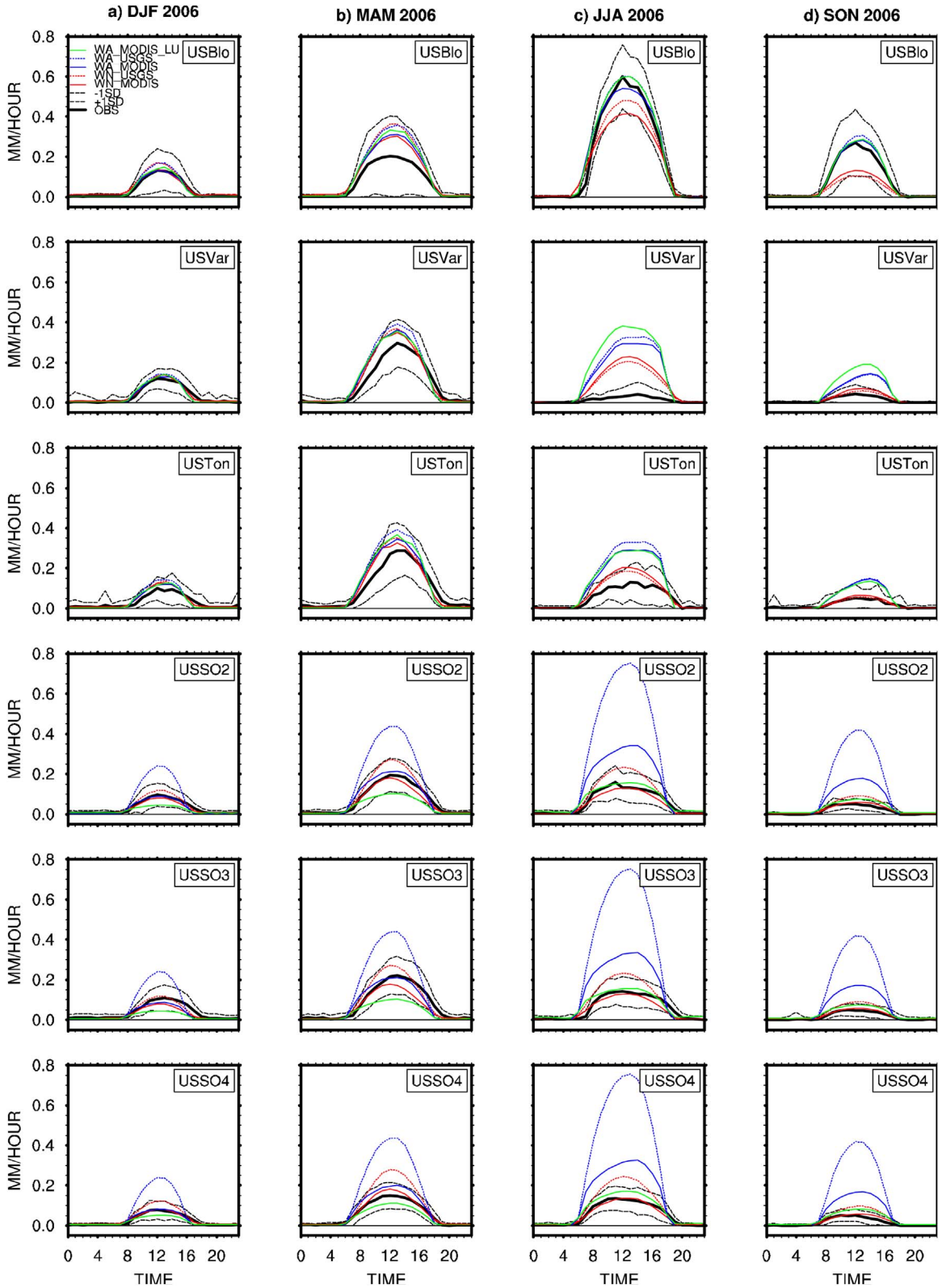

Fig. 9. Diurnal patterns of the actual ET for the six AmeriFlux sites for year 2006. Red, blue, and green lines are WRF-Noah, WRF-ACASA, and WRF-ACASA with PFT correction, black is observation. Color dash and solid lines are for USGS and MODIS respectively. Dash black lines are for ± 1SD of observation.

between the different models and LAI datasets are not statistically significant.

The choices of LAI datasets do not have large impacts on model results of ETo when the same land surface model is used. The differences in annual cumulative reference evapotranspiration over the entire domain using the two LAI datasets simulated by WRF-ACASA and WRF-NOAH are showed in Fig. 7. The differences in ETo simulations with WRF-Noah overlap with the differences in LAI values between the MODIS and USGS dataset such as over the Northern California region as showed in Fig. 1. WRF-ACASA simulations also show differences in the

Table 2
RMSE (mm/day) of actual evapotranspiration, ETa, from the two LAI datasets (USGS and MODIS) and PFT correction (WRF-ACASA LU using MODIS LAI) for the AmeriFlux sites.

Site	WRF-Noah USGS	WRF-Noah MODIS	WRF-ACASA USGS	WRF-ACASA MODIS	WRF-ACASA LU
USBlo	1.25	0.98	0.88	0.71	0.80
USVar	1.09	1.16	1.62	1.47	1.88
USTon	0.62	0.61	1.25	1.03	1.07
USSO2	0.67	0.32	3.04	1.14	0.52
USSO3	0.59	0.32	2.95	1.11	0.57
USSO4	0.80	0.34	3.13	1.12	0.45

same Northern California regions, however, there are more complexity in the overall differences in ETo between the two LAI datasets. In the central and southern regions of California, where plants are more adapted to low moisture environment, small differences in LAI between the two datasets have larger impact on WRF-ACASA than on WRF-Noah. There is a large decrease in ETo over the Los Angeles area with MODIS and WRF-ACASA simulation. This is due to the assumption that over urban grid cells when LAI is lower in MODIS than in USGS larger portion of the area is cover by impermeable urban surface. These differences are more results of variation in model complexity than the choice of LAI dataset.

The Taylor diagram in Fig. 8 illustrates the relative accuracy of the WRF-ACASA and WRF-Noah models to the observational data for daily ETo, 2 m temperature, dew point temperature, wind speed and solar radiation in each of the four seasons. Using three non-dimensional statistical parameters (the ratio of the variances, the correlation between the two fields, and the RMSE), the Taylor diagram quantifies how well each model simulates an observed meteorological field with each LAI dataset. Even though the differences in the LAI values shown in Fig. 1 are large, the impact of LAI on surface variables appears small. The largest impact is from model complexity. Generally in all four seasons, the 2 m air temperatures are well simulated by both WRF-ACASA and WRF-Noah models. However, both models are comparatively poor at simulating wind speed throughout the year. This disparity in wind speed simulation could be due to the difference measurement heights and more general model and station discretization. In the models, wind speeds are simulated at several possible heights. For the CIMIS sites, the 10 m height simulations were used to extrapolate 2 m observations, using Eq. (5). Despite the empirical relationship used to estimate the 2 m wind speed from the simulated 10 m wind speed values, the correlations are still low (Allen et al., 2005).

$$u_2 = u_z\left(\frac{4.87}{\ln(67.8{\cdot}z - 5.42)}\right) \tag{5}$$

During the winter, the ETo simulations from both models have reasonable correlations with the surface observations but the RMSEs are high with a large amount of variability in the standard deviations. This could be due to the bias from the wind speed and dew point temperature simulations used in the Penman-Monteith equation to calculate ETo. The reduction in both dew point temperature variability and RMSE of wind speed during the spring seems to improve ETo simulations. The sudden reduction across all statistical variables during the summer in the ETo simulations seems to be caused by the poor performance of net downward shortwave radiation.

3.2. Actual evapotranspiration

Fig. 9 shows the seasonal diurnal patterns of ETa of the four WRF simulations and WRF-ACASA with PFT correction for the six AmeriFlux stations. While the differences in model complexity and leaf area index data do not have major influence on ETo, the ETa graphs show otherwise. The measured leaf area index in the MODIS LAI dataset systematically lowers the simulated actual evapotranspiration for all six AmeriFlux stations throughout the seasons. This improved LAI helped to reduce the RMSE of model simulation throughout most of the sites and seasons for both WRF-Noah and WRF-ACASA (Table 2). This improvement is larger on the WRF-ACASA model (1.05 mm/day) than the WRF-Noah model (0.21 mm/day). WRF-ACASA relies on LAI in multiple processes and layers: in the radiation transfer equations, as a direct multiplier of the physiologically determined latent energy flux density

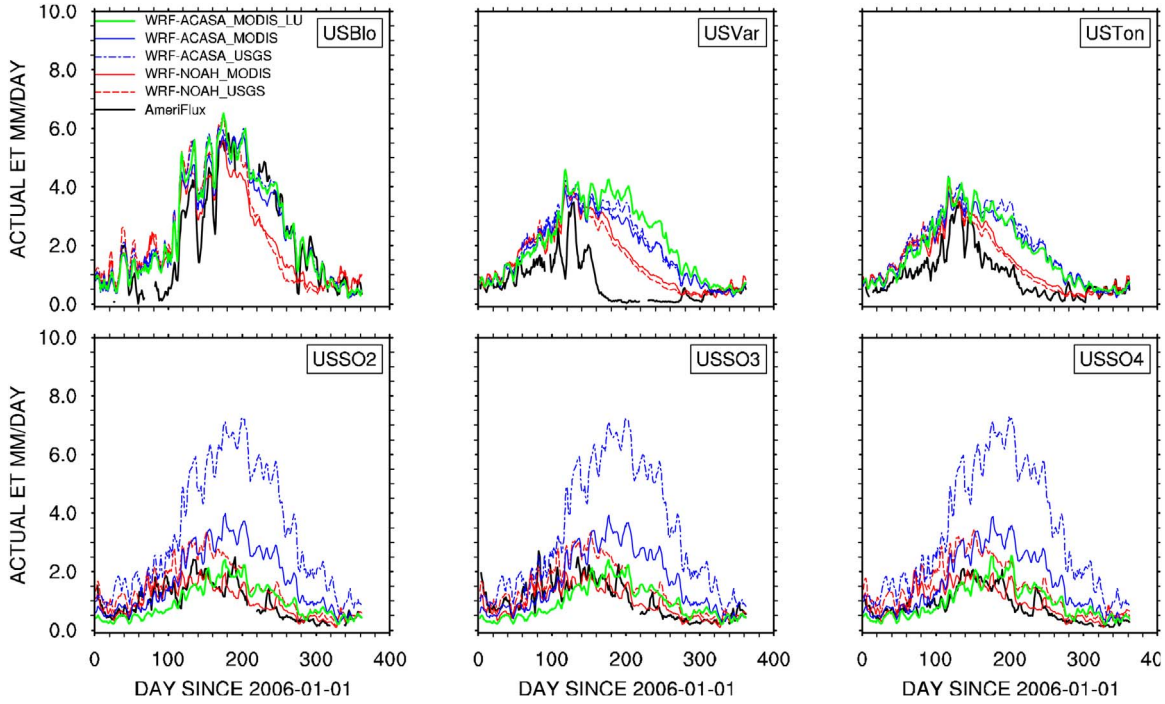

Fig. 10. The time series of cumulative daily ETa for the six AmeriFlux sites during 2006. The black lines are surface measurement of daily ETa, the blue lines are WRF-ACASA simulations, and the red lines are WRF-Noah simulations. The green lines are WRF-ACASA simulation with PFT corrections. The model simulations with MODIS LAI are presented using solid lines and the dash lines are WRF models with USGS LAI.

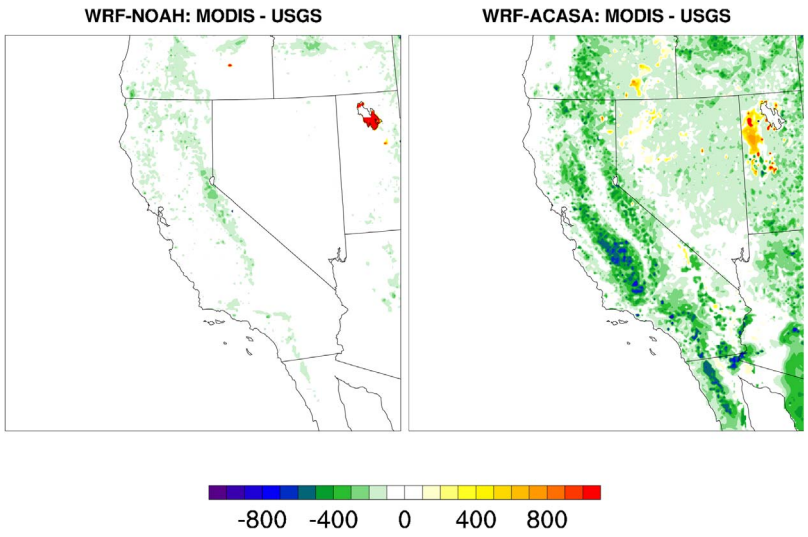

Fig. 11. Maps of cumulative differences in ETa (mm/yr) between MODIS and USGS simulated by WRF-ACASA and WRF-Noah for 2006. The left panel is WRF-Noah and the right panel is WRF-ACASA simulation.

per leaf class, and as multipliers to the leaf drag elements affecting the simulated turbulence. The single layer and simplified processes of Noah model uses the LAI only to reduce the canopy resistance through an inverse relationship. In addition to LAI, PFT plays an important role in the high-complexity WRF-ACASA model. At the Sky Oaks sites, the combination of the PFT mismatch and higher LAI in the USGS LAI dataset drive WRF-ACASA to overestimate ETa. Although the more accurate MODIS LAI greatly reduce the bias, the PFT still has a considerable effect, especially over summer and fall seasons. In effort to correct the PFT bias, the PFT of the WRF grid cell, where the Sky Oak sites are located, is reassigned from Evergreen Needleleaf Forest to shrubland to match the Sky Oak 3 and Sky Oak 4 sites. The green lines in both Fig. 9 shows the updated WRF-ACASA ETa diurnal cycle for the two sites using MODIS LAI. The improvement of PFG-correction in WRF-ACASA is more noticeable than the improvement in LAI representation with the RMSE reduction of 1.26 mm/day when compares to WRF-ACASA with USGS.

Fig. 10 shows the time series of daily cumulative ETa from all five WRF model runs and the AmeriFlux measurements. Similar to Fig. 9, the time series again show the impacts of the model complexity and canopy structure on the actual evapotranspiration simulations. Over the Blodgett forest, where PFTs from the model and surface observation match well, the more complex WRF-ACASA model generally outperforms the WRF-Noah model. The tall and dense canopy of the Blodgett forest is ideal for using the multilayer structure of the WRF- ACASA model. The complex canopy representation and their plant physiological processes more accurately describe the light penetration and inter-canopy mixing, exhibited a better ETa simulation. The same does not apply to the Tonzi Ranch due to underestimation of canopy openness when the WRF-ACASA model assumes horizontal homogeneity of closed forest in each grid cell. Because the Vaira Ranch is closely located to the Tonzi Ranch, they share the same grid cell. The observed ETa at the Vaira site shows a large drop to near zero from June until Fall because the grassland growing season is confined only to the wet season from October to early May. Therefore, the Ameriflux data showed a high ETa during late fall through the spring but low ETa during the remainder of the season when the soil moisture was mostly used up. However, both WRF-ACASA and WRF-Noah do not include the short season of grass, where soil moisture limits vegetation grow. Hence, both models overestimated the ETa outside of the growing season for the Vaira Ranch site. Sites with deeper rooted vegetation also showed some effect of insufficient soil moisture but to a lesser extent than the shallow rooted grass at Vaira. The differences in surface conditions and vegetation types of the Vaira Ranch and Tonzi Ranch sites resulted in very different ETa values even though they are close to each other, thus sharing the same model grid cell. Improvement in both PFT and LAI greatly increase the agreement between the WRF-ACASA simulations and observations as seen in Table 2. The correct PFT affects the microclimate, so the more accurate PFT means the microclimate is more accurate and the simulated ETo should be more accurate. However, there will still be discrepancies between the different models' ability to simulate ETo. Net radiation, air temperature and relative humidity are the main variables that affect ETo, and the more accurate WRF-ACASA tends to simulate these values more accurately than the WRF-NOAH type models. The impact of PFT reassignment for the Sky Oak site on WRF-Noah is negligible compared to the impact on WRF-ACASA, thus it is not shown.

The maps of annual cumulative difference of ETa between the MODIS and USGS are shown in Fig. 11 for both WRF-ACASA and WRF-Noah. There are large differences in the WRF-ACASA simulations between the two LAI datasets, however these differences are less pronounced in the WRF-Noah simulations. The largest differences in ETa occur over the Central Valley and Northern California, which align closely with the differences in LAI shown in Fig. 1. This is expected, since LAI is essential in several processes in the WRF-ACASA model. In contrast, the WRF-Noah model only uses LAI in the scaling of the canopy resistance. Therefore, an overestimate of LAI in the USGS dataset would result in WRF-ACASA to overestimate ETa more than WRF-Noah.

The Taylor diagram in Fig. 12 summarizes the actual evapotranspiration performances of the five simulations over the six AmeriFlux sites using WRF-ACASA with USGS, WRF-ACASA with MODIS, and WRF-ACASA with MODIS and PFT bias correction, WRF-Noah with USGS, and WRF-Noah with MODIS. The figure shows that the impacts of LAI on land surface models depend on the complexity of the model. While the effect of LAI is to improve ETa simulations in both WRF-ACASA and WRF-Noah, the high complexity WRF-ACASA model benefits the most from the increase in leaf area index accuracy. For example, WRF-ACASA simulations using USGS LAI show poor correlations with surface observation during summer (JJA) and fall (SON). The RMSE for the simulated ETa during the summer season is too high and outside of the graph, therefore WRF-ACASA with USGS LAI is not displayed on the Taylor diagram during the summer season. However, when MODIS LAI is used to improve the surface representation, the ETa simulations also improved. The medium complexity WRF-Noah model shows much smaller improvements of ETa when using MODIS LAI than the WRF-ACASA model. Furthermore, correcting the grid cell PFT in WRF over Sky Oak 3 and Sky Oak 4 sites to match the observed PFTs, ETa simulations from WRF-ACASA with MODIS LAI vastly improve during summer (JJA) and fall (SON) seasons when compared with surface observation.

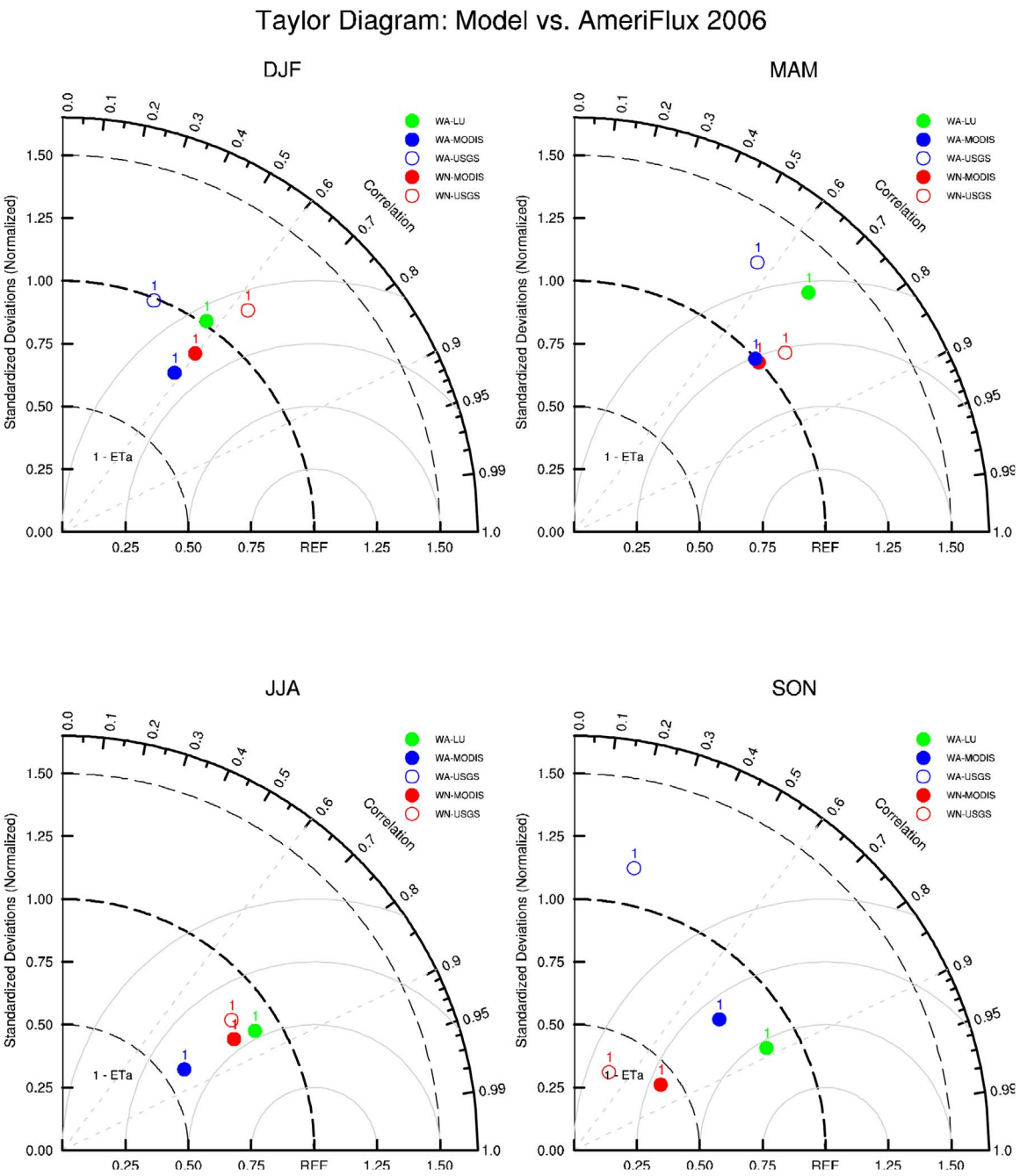

Fig. 12. Seasonal Taylor diagram for model simulations and surface measurements of ETa over six AmeriFlux sites for 2006. Blue circle is WRF-ACASA with USGS LAI, blue solid dot is WRF-ACASA with MODIS LAI; red circle is WRF-Noah with USGS, red solid dot is WRF-Noah with MODIS; green solid dot is WRF-ACASA with MODIS LAI and PFT bias correction. Winter is DJF (December, January, February), spring is MAM (March, April, May), summer is JJA (June, July, August), and fall is SON (September, October, November).

The sensitivities of LAI and PFT in WRF simulations using ACASA versus Noah are due to the differences in surface representation between the WRF-ACASA and WRF-Noah models. Unlike the single layer "big leaf" model of the WRF-Noah, each of the plant functional types in the WRF-ACASA model is associated with a different multilayer canopy structure. While the representation of each PFT with specific canopy structures and plant physiological process allows a more realistic surface representation, these complex relationships are more dependent on the quality of input variables such as land cover type and leaf area index. For example, the model PFT identifies Sky Oaks sites as physiologically active (throughout the year) evergreen needle leaf forest, when in reality they are low-LAI, seasonally inactive, vegetated savanna and scrublands. This affects physiological processes in WRF-ACASA, causing overestimation of ETa; however, the single-layer WRF-Noah relies less on the land cover representation and is therefore less sensitive to changes in land surface type designation. Improvements in surface representation of LAI and PFT help increase the accuracy of the high complexity WRF-ACASA model more than the medium complexity WRF-Noah model.

4. Summary and conclusion

In this study, the mesoscale model WRF is used to simulate ETo and ETa for locations with different combinations of two land surface models and two LAI datasets to examine the impacts that surface representations and model complexity have on ETo and ETa. The two land surface models are the intermediate complexity Noah land surface model and high complexity ACASA model. The two LAI datasets used in

the models are from the USGS and MODIS. There are four model simulations: WRF-ACASA with USGS LAI, WRF-ACASA with MODIS LAI, WRF-Noah with USGS LAI, and WRF-Noah with MODIS LAI, plus an addition ETa simulation using WRF-ACASA with MODIS LAI and PFT bias correction. Each simulation was run for the years 2005 and 2006 over all of California and adjacent terrain, but only results from 2006 are shown.

The model results were evaluated using surface observations from the 120 CIMIS network stations for ETo and from the six AmeriFlux stations for both ETo and ETa. Sensitivity tests were employed to evaluate the impacts of differences in surface representations (in both LAI and PFT) and model complexity on simulated ETo and ETa in diverse environmental conditions. The results from these four simulations show that an increase in leaf area index accuracy generally improves estimates of ETa for both the WRF-ACASA and WRF-Noah models, but it has little effect on ETo. The Taylor diagrams for CIMIS stations and AmeriFlux stations do not show significant improvement in ETo or other meteorological variables with improved LAI. There is, however, a small improvement of ETo in the WRF-ACASA when MODIS LAI is used instead of the USGS LAI. In addition to LAI, the land use cover or PFT also impacts on simulations of ETa. When PFTs are bias corrected to match surface observation and model assumption, the ETa simulations in the high complexity WRF-ACASA increase and agree well with surface observations. In the high complexity WRF-ACASA model, the plant functional type determines the multilayer canopy structure as well as plant physiological parameters. As a result, it is more sensitive to the land cover type than the single-layer WRF-Noah model.

In conclusion, surface representations such as LAI and PFT appear to impact the detailed plant physiological processes calculations such as ETa. How the overall representation affects surface processes, however, depends on the model complexity. As the model complexity increases, the model sensitivity to surface representation also increases. The surface processes of the WRF-ACASA model are more sensitive to the leaf area index than the simple, single layer WRF-Noah model. The WRF-ACASA model is also sensitive to land use cover, whereas the WRF-Noah model is not.

While the high complexity of WRF-ACASA increases the realism of the plant physiological processes, it must be coupled with high accuracy in land surface representation in both leaf area index and land use cover. Consequently, there is a linear relationship between the model complexity and data quality in surface representation. The lower complexity land surface model is less restricted, thus providing more flexibility when high accuracy data is not available. Higher complexity models, however, perform better over more diverse ecosystems such as forests. Depending on the target variables and study areas of interest, the model complexity and surface representation requirements vary.

Further improvement in simulating surface processes such as evapotranspiration can be achieved by improving the model grid cell representation. Both WRF-ACASA and WRF-Noah models assume one dominant plant functional type in each grid cell. The AmeriFlux data, then again, show that such homogeneous representation of PFT is inaccurate. Instead of using only one dominant PFT in each grid cell, future simulations of land surface processes can be improved by using a combination of PFTs in each grid cell. Although the impact of heterogeneous land use cover in each grid cell may not greatly affect low- or even moderate-complexity models such as WRF-Noah, it could benefit high-complexity models such as the WRF-ACASA model.

Acknowledgments

This work is supported in part by the National Science Foundation under Awards No. ATM-0619139 and EF-1137306. The Joint Program on the Science and Policy of Global Change is funded by a number of federal agencies and a consortium of 40 industrial and foundation sponsors. (For the complete list see http://globalchange.mit.edu/sponsors/current.html).

References

Abramowitz, G., Leuning, R., Clark, M., Pitman, A., 2008. Evaluating the performance of land surface models. J. Climate 21 (21), 5468–5481.
Allen, R., Walter, I., Elliott, R., Howell, T., Itenfisu, D., Jensen, M., Snyder, R., 2005. The ASCE standardized reference evapotranspiration equation, American Society of Civil Engineers.
Bounoua, L., Collatz, G., Los, S., Sellers, P., Dazlich, D., Tucker, C., Randall, D., 2000. Sensitivity of climate to changes in NDVI. J. Climate 13 (13), 2277–2292.
Chase, T., Pielke, R., Kittel, T., Nemani, R., Running, S., 1996. Sensitivity of a general circulation model to global changes in leaf area index. J. Geophys. Res. 101, 7393–7408.
Chen, S., Dudhia, J., 2000. Annual Report WRF Physics. Air Force Weather Agency (Tech. rep.).
Chen, F., Dudhia, J., 2001a. Coupling an advanced land surface-hydrology model with the Penn State-NCAR MM5 modeling system. Part I: model implementation and sensitivity. Mon. Weather. Rev. 129 (4), 569–585.
Chen, F., Dudhia, J., 2001b. Coupling an advanced land surface-hydrology model with the Penn State-NCAR MM5 modeling system. Part II: preliminary model validation. Mon. Weather Rev. 129 (4), 587–604.
Chen, S., Sun, W., 2002. A one-dimensional time dependent cloud model. J. Meteor. Soc. Japan 80 (1), 99–118.
Chen, F., Janjic, Z., Mitchell, K., 1997. Impact of atmospheric surface-layer parameterizations in the new land-surface scheme of the NCEP mesoscale Eta model. Bound. Layer Meteorol. 85 (3), 391–421.
Collatz, G., Ball, J., Grivet, C., Berry, J., 1991. Physiological and environmental regulation of stomatal conductance, photosynthesis and transpiration: a model that includes a laminar boundary layer. Agric. For. Meteor. 54 (2), 107–136.
Dickinson, R., Henderson-Sellers, A., 2006. Modelling tropical deforestation: a study of GCM land-surface parametrizations. Q. J. R. Meteor. Soc. 114 (480), 439–462.
Dirmeyer, P., Niyogi, D., de Noblet-Ducoudre, N., Dickinson, R., Snyder, P., 2010. Impacts of land use change on climate. Int. J. Climatol. 30 (13), 1905–1907.
Dudhia, J., 1989. Numerical study of convection observed during the winter monsoon experiment using a mesoscale two-dimensional model. J. Atmos. Sci. 46 (20), 3077–3107.
Farquhar, G., Von Caemmerer, S., 1982. et al., Modelling of photosynthetic response to environmental conditions. In: In: Lange, O., Nobel, P., Osmond, C., Ziegler, H. (Eds.), Encyclopedia of Plant Physiology 12. pp. 549–587.
Gao, X., Dirmeyer, P., Guo, Z., Zhao, M., 2008. Sensitivity of land surface simulations to the treatment of vegetation properties and the implications for seasonal climate prediction. J. Hydrol. 9 (3), 348–366.
Gutman, G., Ignatov, A., 1998. The derivation of the green vegetation fraction from NOAA/AVHRR data for use in numerical weather prediction models. Int. J. Climatol. 19 (8), 1533–1543.
Hales, K., Neelin, J., Zeng, N., 2004. Sensitivity of tropical land climate to leaf area index: role of surface conductance versus albedo. J. Climate 17 (7), 1459–1473.
Henderson-Sellers, A., McGuffie, K., Pitman, A., 1996. The project for intercomparison of land-surface parametrization schemes (PILPS): 1992–1995. Clim. Dyn. 12 (12), 849–859.
Hong, S., Pan, H., 1996. Nonlocal boundary layer vertical diffusion in a medium-range forecast model. Mon. Weather Rev. 124 (10), 2322–2339.
Houborg, R., Soegaard, H., 2004. Regional simulation of ecosystem CO2 and water vapor exchange for agricultural land using NOAA AVHRR and Terra MODIS satellite data. Application to Zealand Denmark. Remote Sens. Environ. 93 (1), 150–167.
Jacquemin, B., Noilhan, J., 1990. Sensitivity study and validation of a land surface parameterization using the HAPEX-MOBILHY data set. Bound. Layer Meteorol. 52 (1), 93–134.
Jones, H., 1992. Plants and Microclimate: A Quantitative Approach to Environmental Plant Physiology. Cambridge University Press.
Knyazikhin, Y., Glassy, J., Privette, J., Tian, Y., Lotsch, A., Zhang, Y., Wang, Y., Morisette, J., Votava, P., Myneni, R., et al., 1999. MODIS Leaf Area Index (LAI) and Fraction of Photosynthetically Active Radiation Absorbed by Vegetation (FPAR) Product (MOD15) Algorithm Theoretical Basis Document. NASA Goddard Space Flight Center, Greenbelt, MD (Tech. rep.).
Leuning, R., 1990. Modelling stomatal behaviour and photosynthesis of eucalyptus grandis. Aust. J. Plant Physiol. 17 (2), 159–175.
Levitt, J., et al., 1980. Responses of Plants to Environmental Stresses. Volume II. Water, Radiation, Salt, and Other Stresses, ed. 2. Academic Press (no.).
Mahrt, L., Ek, M., 1984. The influence of atmospheric stability on potential evaporation. J. Climate Appl. Meteor. 23, 222–234. http://dx.doi.org/10.1175/1520-0450(1984)023<0222:TIOASO>2.0.CO;2.
Mesinger, F., DiMego, G., Kalnay, E., Mitchell, K., Shafran, P., Ebisuzaki, W., Jovic, D., Woollen, J., Rogers, E., Berbery, E., Ek, M., Fan, Y., Grumbine, R., Higgins, W., Li, H., Lin, Y., Manikin, G., Parrish, D., Shi, W., 2006. North American regional reanalysis. Bull. Am. Meteor. Soc. 87 (3), 343–360. http://dx.doi.org/10.1175/BAMS-87-3-343.
Meyers, T., Paw U, K., 1987. Modelling the plant canopy micrometeorology with higher-order closure principles. Agric. For. Meteor. 41 (1), 143–163.
Meyers, T., 1985. A Simulation of the Canopy Microenvironment Using Higher Order Closure Principles, Ph.D Thesis. Purdue University.
Mlawer, E., Taubman, S., Brown, P., Iacono, M., Clough, S., 1997. Radiative transfer for inhomogeneous atmospheres: RRTM, a validated correlated-k model for the long-wave. J. Geophys. Res. 102 (D14), 16663–16682. http://dx.doi.org/10.1029/97JD00237.
Pitman, A., Zhao, M., Desborough, C., 1999. Investigating the sensitivity of a land surface schemes simulation of soil wetness and evaporation to spatial and temporal leaf area

index variability within the Global Soil Wetness Project. J. Meteor. Soc. Japan 77, 281–290.
Potter, C., Randerson, J., Field, C., Matson, P., Vitousek, P., Mooney, H., Klooster, S., 1993. Terrestrial ecosystem production: a process model based on global satellite and surface data. Global Biogeochem. Cycles 7 (4), 811–841.
Pyles, R., Weare, B., Paw I, K., 2000. The UCD Advanced Canopy-Atmosphere-Soil Algorithm: comparisons with observations from different climate and vegetation regimes. Q. J. R. Meteor. Soc. 126, 2951–2980.
Pyles, P., 2000. The Development and Testing of the UCD Advanced Canopy–Atmosphere–Soil Algorithm (ACASA) for Use in Climate Prediction and Field Studies, Ph.D. Thesis. University of California, Davis.
Su, H., Paw U, K., Shaw, R., 1996. Development of a coupled leaf and canopy model for the simulation of plant-atmosphere interactions. J. Appl. Meteor. 35, 733–748.
Xu, L., Pyles, R., Paw, U., Chen, S.-H., Monier, E., 2014. Coupling the high complexity land surface model acasa to the mesoscale model wrf. Geosci. Model Dev. 7, 2917–2932. http://dx.doi.org/10.5194/gmd-7-2917-2014.
Zhan, X., Kustas, W., 2001. A coupled model of land surface CO2 and energy fluxes using remote sensing data. Agric. For. Meteor. 107 (2), 131–152.

Joint Program Reprint Series - Recent Articles

For limited quantities, Joint Program publications are available free of charge. Contact the Joint Program office to order.
Complete list: http://globalchange.mit.edu/publications

2017-9 Impact of Canopy Representations on Regional Modeling of Evapotranspiration using the WRF-ACASA Coupled Model. Xu, L., R.D. Pyles, K.T. Paw U, R.L. Snyder, E. Monier, M. Falk and S.H. Chen, *Agricultural and Forest Meteorology*, 247: 79–92 (2017)

2017-8 The economic viability of Gas-to-Liquids technology and the crude oil-natural gas price relationship. Ramberg, D.J., Y.-H.H. Chen, S. Paltsev and J.E. Parsons, *Energy Economics*, 63: 13–21 (2017)

2017-7 The Impact of Oil Prices on Bioenergy, Emissions and Land Use. Winchester, N. and K. Ledvina, *Energy Economics*, 65(2017): 219–227 (2017)

2017-6 The impact of coordinated policies on air pollution emissions from road transportation in China. Kishimoto, P.N., V.J. Karplus, M. Zhong, E. Saikawa, X. Zhang and X. Zhang, *Transportation Research Part D*, 54(2017): 30–49 (2017)

2017-5 Twenty-First-Century Changes in U.S. Regional Heavy Precipitation Frequency Based on Resolved Atmospheric Patterns. Gao, X., C.A. Schlosser, P.A. O'Gorman, E. Monier and D. Entekhabi, *Journal of Climate*, online first, doi: 10.1175/JCLI-D-16-0544.1 (2017)

2017-4 The CO_2 Content of Consumption Across U.S. Regions: A Multi-Regional Input-Output (MRIO) Approach. Caron, J., G.E. Metcalf and J. Reilly, *The Energy Journal*, 38(1): 1–22 (2017)

2017-3 Human Health and Economic Impacts of Ozone Reductions by Income Group. Saari, R.K., T.M. Thompson and N.E. Selin, *Environmental Science & Technology*, 51(4): 1953–1961 (2017)

2017-2 Biomass burning aerosols and the low-visibility events in Southeast Asia. Lee, H.-H., R.Z. Bar-Or and C. Wang, *Atmospheric Chemistry & Physics*, 17, 965–980 (2017)

2017-1 Statistical emulators of maize, rice, soybean and wheat yields from global gridded crop models. Blanc, É., *Agricultural and Forest Meteorology,* 236, 145–161 (2017)

2016-25 Reducing CO_2 from cars in the European Union. Paltsev, S., Y.-H.H. Chen, V. Karplus, P. Kishimoto, J. Reilly, A. Löschel, K. von Graevenitz and S. Koesler, *Transportation*, online first (doi:10.1007/s11116-016-9741-3) (2016)

2016-24 Radiative effects of interannually varying vs. interannually invariant aerosol emissions from fires. Grandey, B.S., H.-H. Lee and C. Wang, *Atmospheric Chemistry & Physics,* 16, 14495–14513 (2016)

2016-23 Splitting the South: China and India's Divergence in International Environmental Negotiations. Stokes, L.C., A. Giang and N.E. Selin, *Global Environmental Politics*, 16(4): 12–31 (2016)

2016-22 Teaching and Learning from Environmental Summits: COP 21 and Beyond. Selin, N.E., *Global Environmental Politics*, 16(3): 31–40 (2016)

2016-21 Southern Ocean warming delayed by circumpolar upwelling and equatorward transport. Armour, K.C., J. Marshall, J.R. Scott, A. Donohoe and E.R. Newsom, *Nature Geoscience* 9: 549–554 (2016)

2016-20 Hydrofluorocarbon (HFC) Emissions in China: An Inventory for 2005–2013 and Projections to 2050. Fang, X., G.J.M. Velders, A.R. Ravishankara, M.J. Molina, J. Hu and R.G. Prinn, *Environmental Science & Technology*, 50(4): 2027–2034 (2016)

2016-19 The Future of Natural Gas in China: Effects of Pricing Reform and Climate Policy. Zhang, D. and S. Paltsev, *Climate Change Economics*, 7(4): 1650012 (2016)

2016-18 Assessing the Impact of Typhoons on Rice Production in the Philippines. Blanc, É. and E. Strobl, *Journal of Applied Meteorology and Climatology,* 55: 993–1007 (2016)

2016-17 Uncertainties in Atmospheric Mercury Modeling for Policy Evaluation. Kwon, S.Y. and N.E. Selin, *Current Pollution Reports,* 2(2): 103–114 (2016)

2016-16 Limited Trading of Emissions Permits as a Climate Cooperation Mechanism? US-China and EU-China Examples. Gavard, C., N. Winchester and S. Paltsev, *Energy Economics,* 58(2016): 95–104 (2016)

2016-15 Interprovincial migration and the stringency of energy policy in China. Luo, X., J. Caron, V.J. Karplus, D. Zhang and X. Zhang, *Energy Economics,* 58(August 2016): 164–173 (2016)

2016-14 Modelling the potential for wind energy integration on China's coal-heavy electricity grid. Davidson, M.R., D. Zhang, W. Xiong, X. Zhang and V.J. Karplus, *Nature Energy,* 1: 16086 (2016)

2016-13 Pathways to Mexico's climate change mitigation targets: A multi-model analysis. Veysey, J., C. Octaviano, K. Calvin, S. Herreras Martinez, A. Kitous, J. McFarland and B. van der Zwaan, *Energy Economics,* 56(May): 587–599 (2016)

2016-12 Uncertainty in future agro-climate projections in the United States and benefits of greenhouse gas mitigation. Monier, E., L. Xu and R. Snyder, *Environmental Research Letters*, 11(2016): 055001 (2016)

MIT Joint Program on the Science and Policy of Global Change

Massachusetts Institute of Technology
77 Massachusetts Ave., E19-411
Cambridge MA 02139-4307 (USA)

T (617) 253-7492 F (617) 253-9845
globalchange@mit.edu
http://globalchange.mit.edu